Edge Sheared Flows and Blob Dynamics

J. R. Myra,[a] W. M. Davis,[b] D. A. D'Ippolito,[a] B. LaBombard,[c]
D. A. Russell,[a] J. L. Terry,[c] and S. J. Zweben,[b]

[a] Lodestar Research Corporation, Boulder, CO, USA
[b] Princeton Plasma Physics Laboratory, Princeton, NJ, USA
[c] Massachusetts Institute of Technology, Cambridge MA, USA

E-mail contact of main author: jrmyra@lodestar.com

Abstract. The dynamics of blob-filaments in the strongly radially inhomogeneous edge and scrape-off-layer (SOL) region of a tokamak plasma is considered, with emphasis on sheared flow generation and interaction. Both numerical simulations and experimental data analysis are employed. The simulations use the fluid-based 2D curvature-interchange model embedded in the SOLT code. A blob-tracking algorithm based on 2D time-resolved images from the gas puff imaging diagnostic has also been developed and applied to NSTX, Alcator C-Mod and simulation data. The algorithm is able to track the blob motion and changes in blob structure, such as elliptical deformations, that can be affected by sheared flows. Results of seeded blob simulations are compared with the experimental data to determine the role of plasma parameters on the blob tracks and to evaluate the exchange of momentum between the blobs and flows. Seeded blob simulations are shown to reproduce many qualitative and quantitative features of the data including size, scale-length and direction of perpendicular (approximately poloidal) flows, the inferred Reynolds forces, poloidal reversal of blob tracks, and blob trapping and/or ejection. Mechanisms related to blob motion, SOL currents and radial inhomogeneity are shown to be sufficient to explain the presence or absence of mean sheared flows in selected shots.

1. Introduction

Sheared flows play an important role in regulating turbulence in fusion plasmas. [1] Furthermore, it has been known for some time that radial inhomogeneity provides a mechanism for sheared flow generation by the turbulence [2,3]. Here, we consider the interaction of edge sheared flows with coherent turbulent structures in the edge and scrape-off-layer (SOL), i.e. blob-filaments, [4,5], focusing on the generation of flows, the dynamics of the blob-filaments and their mutual interaction. We define a blob-filament (or "blob") to be any filamentary field-aligned structure of significantly enhanced pressure in the edge or SOL region. Because coherent structures are readily observed in the edge plasma using diagnostics such as gas puff imaging (GPI) [6], the present approach enables a new kind of comparison of edge turbulence theory with data.

The work is motivated by several considerations. Edge sheared flows are believed to be important for the L-H, and H-L transitions, and improved understanding of their role will be required for first-principles scalings of these transitions for ITER and future devices. Blob generation and dynamics impact both the (near-separatrix) SOL width critical for ITER power handling in the divertor [7], and far SOL interaction with plasma-facing components, which is also an important concern.

This paper describes both reduced model simulations and experimental data analysis. The simulations employ a fluid-based 2D curvature-interchange model embedded in the SOLT code [8]. Previous simulations with the SOLT code in various regimes have demonstrated the dramatic effect of sheared binormal (approximately poloidal) flows on edge turbulence, and

the generation of mesoscale (blob) structures. Simulations [9] with sheared flows completely suppressed led to the generation of radial streamers. Normally, sheared zonal flows develop by self-consistent Reynolds stress interactions. In such simulations using L-mode-like parameters, radial streamers were converted to discrete blob structures when the shearing rate was strong enough to dominate the linear growth rate [8], i.e. when mean flows significantly mitigate the nonlinear transport flux. Furthermore, in simulations [8,10] using NSTX L-mode parameters, zonal flow relaxation oscillations, coherently coupled to the transport flux, were observed in a frequency range similar to that seen in analysis of GPI data which examined quiet periods preceding the L-H transition [10,11]. Finally, when even stronger binormal flows were applied artificially to simulate H-mode discharges on NSTX, [12] blobs were suppressed, qualitatively in accord with other NSTX experimental data [13]. Related work has also recently been reported by other authors [14,15] who have considered the impact of sheared flows on blobs and eddies and the relation of these to the confinement regime.

In this paper, we seek insight into the underlying mechanisms for sheared flow generation and interaction with blob-filaments from the comparison of blob simulations with data. Our task is greatly facilitated by a new analysis tool for tracking the motion and changes in structure of blobs [16], namely, a blob-tracking algorithm based on 2D time-resolved images from the GPI diagnostic. This tool and sample results are discussed in Sec. 2. In Sec. 3 we consider some mechanisms for the generation of flows that are related to blob motion, SOL currents and radial inhomogeneity. The SOLT code simulation model is described in Sec. 4 together with trajectories of seeded blob simulations for parameters relevant to an NSTX shot. Qualitative agreement with experimental data can be inferred. A detailed quantitative comparison of model results with experimental results from NSTX and Alcator C-Mod is given. Finally, our conclusions are given in Sec. 5.

2. Gas-Puff Imaging and Tracking of Blob Trajectories

Gas-puff imaging is a valuable diagnostic for the detection of edge turbulent structures and the analysis of their motion. A detailed description of the diagnostic is given elsewhere. [6] The basic idea is that a small amount of neutral gas (usually deuterium or helium) is puffed into the edge plasma at a particular toroidal location. The line emission from the gas, which depends on the local plasma density and temperature, is then detected and recorded by a high framing rate camera. In the present study, the camera is positioned to view the motion of the turbulent structures in the plane perpendicular to the magnetic field B. In the present datasets, a 64x64 pixel GPI image frame was captured every 2.5 μs for a total of 20 ms.

A sample processed frame from Alcator C-Mod is shown in Fig. 1 for the normalized GPI intensity, i.e. the local intensity I(x, y, t) normalized to the time averaged intensity $\langle I(x, y)\rangle_t$. For each local maximum in the frame meeting specified filtering criteria, an ellipse is fit to the half-maximum contour level. The motion of the central maximum and changes in the elliptical fit are tracked from frame to frame. [16] The allowed displacement of a given turbulent structure between frames is restricted (typically to 10 pixels) to distinguish different structures. The structure is considered to be a blob if it meets these criteria and has a sufficient lifetime (typically taken as more that 25 μs). Note that this rather general definition of a blob can include wave crests inside the separatrix as well as isolated filamentary structures that have been ejected into the SOL.

In this paper we analyze two shots from the NSTX and Alcator C-Mod experiments. Parameters for these discharges are give in Table I. Both are Ohmic plasmas; the NSTX case is preheated by neutral beams. Of particular note is the difference in the SOL collisionality

parameter [5] $\Lambda = \nu_{ei}L_{\|}/(\Omega_e\rho_s)$, a point to which we will return. A set of superimposed blob tracks from 3 ms of GPI data in NSTX is shown in Fig. 2. The fitted ellipses (starting one filled) are drawn with the same minor radius regardless of blob size for visual clarity and only a portion of the ~25x25 cm camera image is shown. The separatrix position is shown by a dashed line. Some blob tracks show outward motion (ejection), some are confined to the edge region (here defined as inside the separatrix). The motion of the edge structures is upwards, which corresponds to the electron diamagnetic direction. Some blob tracks show reversal of v_y near the separatrix indicating the action of an accelerating force. The dominant motion in the SOL is downward, in the ion diamagnetic direction. One of the main goals of this paper is to understand and quantify the mechanisms responsible for the observed blob motion in the y (approximately poloidal) direction, i.e. the origin of perpendicular sheared flows.

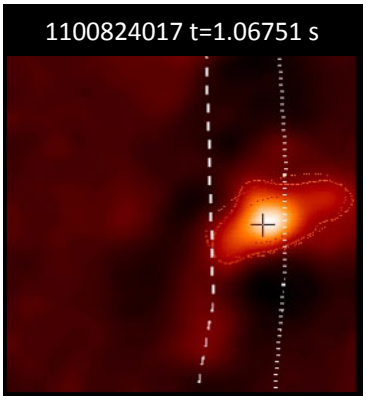

FIG. 1. Sample processed frame of normalized GPI intensity from the Alcator C-Mod shot analyzed in this paper. The camera image is approximately 5.9 cm on a side.

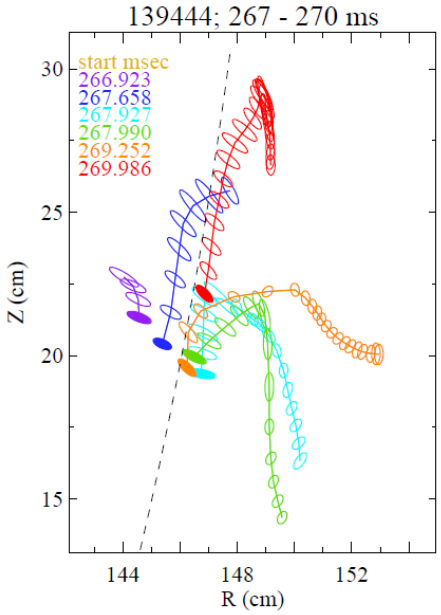

FIG. 2. Sample set of superimposed blob tracks from the NSTX shot.

TABLE I: DISCHARGE PARAMETERS.

	NSTX Shot 139444	C-MOD Shot 1100824017
$n_{e,sep}$ (m^{-3})	5.8×10^{18}	1.0×10^{20}
$T_{e,sep}$ (eV)	19	47
$\rho_{s,sep}$ (cm)	0.26	0.025
$\Lambda_{SOL} \sim \nu_{e*}(m_e/m_i)^{1/2}$	0.3 – 0.8	1 – 3
blob size $\delta_{b,sep}$ (cm)	2.2 ± 0.5	0.4 ± 0.1
$\delta I/\langle I\rangle\|_{sep}$	0 – 1.6	0 – 0.6

3. Mechanisms for the generation of flows and blob motion

Strong radial inhomogeneity present in the edge and SOL region of a tokamak plasma leads to several mechanisms for sheared flow generation and its interaction with turbulence. These mechanisms are related to shearing and rotation or tilting deformations of the turbulent structures (called "blobs" here both inside and outside the separatrix) due to various effects:

1) radial variation of the wave group velocity on the scale of the blob radius due to steep profiles and or rapid changes in topology across the separatrix which shear and rotate the blob charge dipole [4,5], converting radial blob motion into poloidal motion;

2) a net monopole blob potential due to adiabatic electron physics ($\delta n \sim \delta\Phi$) which induces rotation of the blob charge dipole, mixing radial and poloidal blob motion;

3) asymmetry in the positive and negative parallel currents in the SOL (due to the asymmetry of the sheath current-voltage relation) which causes the blob to charge positive and partially rotate, again converting radial motion into poloidal motion; [17]

4) blob rotation as a sheath-connected blob enters the SOL due to finite blob T_e which induces an internal blob radial electric field [18];

5) interaction of the blob with an existing strong E×B shear layer leading to vortex merging and charge dynamics: positive and negative regions of the blob charge dipole are repelled or attracted by regions of vorticity (charge) in the shear layer.

These mechanisms have well-known counterparts in traditional nonlinear Fourier-wave theory [2,3], but it is illuminating to see them at play in the context of coherent blob structures. Moreover, blob structures are readily detectable by the GPI diagnostic enabling an entirely new kind of comparison between theory and experiment.

4. SOLT code simulations of NSTX and Alcator C-Mod discharges

The Scrape-Off-Layer Turbulence (SOLT) code [8] is a fluid code that models turbulence in a two-dimensional region perpendicular to the magnetic field B at the outboard midplane of the torus. SOLT implements classical parallel physics using closure relations [4] for the midplane parallel current and parallel fluxes for collisional regimes ranging from sheath-connected to conduction limited. The SOLT code can describe arbitrarily strong nonlinear plasma dynamics ($\delta n/n \sim 1$), including blob formation, and the physics model supports interchange-type curvature-driven modes, sheath and Kelvin-Helmholtz (KH) instabilities, and drift waves. The present version assumes cold ions. SOLT also includes the self-consistent evolution of zonal (i.e., poloidally-averaged) flows. For comparison with experimental gas GPI data, SOLT employs a synthetic GPI diagnostic to simulate both He and D gas puffs.

SOLT was used for both seeded blob simulations and quasi-steady turbulence simulations of the NSTX and Alcator C-Mod shots. The turbulence simulations, confirm the main conclusions of the seeded blob simulations, and will be discussed in detail in a full length companion paper. The seeded blob simulations were run as a SOLT initial value problem. Smoothed experimental plasma profiles of density and temperature were employed together with other machine parameters that enter the SOLT model: magnetic field B, major radius R, and connection length profile $L_{||}$. Dissipation parameters (plasma viscosity and flow damping) were treated as ad-hoc input parameters since experimental values were not known. Typical blob spatial sizes, amplitudes, and birth locations were extracted from the experimental dataset. A Gaussian blob with the given properties was then superimposed on the back-

ground plasma profiles as an initial condition for the SOLT simulation. The blob was tracked until it either disappeared (lost its structure) or travelled radially to a limiter in the far SOL.

Trajectories for six cases, relevant to the NSTX discharge are shown in Fig. 3. Fig. 3a is a representative NSTX track initializing the blob with the mean blob parameters of Table 1, and using experimental outer midplane plasma profiles and parameters for other simulation inputs, except that no mean background flow is imposed. Thus the v_y of the blob is generated entirely by blob interaction with the plasma and geometry. This track exhibits blob ejection and v_y reversal similar to the some of the experimental tracks of Fig. 2. The inferred size (amplitude) of the radial and poloidal blob velocities in the edge and SOL are within a factor of two of the experimental values, the directions are the same, and the scale lengths of variation are similar. Next in SOLT we artificially varied simulation parameters and physics to infer the importance of specific mechanisms in the experimental data. Fig. 3b illustrates the track for a completely sheath-connected case (zero collisionality), while Fig. 3c is for a completely sheath-disconnected case (large collisionality). We infer that parallel currents in the SOL are important in establishing the blob track and the y-acceleration along the track. Fig. 3d show the result of suppressing electron adiabatic effects, and hence the upward electron drift, in the edge region. This highly-charged (because adiabaticity is neutralizing) blob is ejected rapidly, and moves downward in the SOL due to the asymmetry of the sheath current-voltage relation, which favors electron loss. Figs. 3e and 3f show the result of imposing a mean background ExB flow in the SOL, respectively up in 3e and down in 3f. The counter-shear flow layer in 3e (relative to the net positive charge of the blob) enhances blob ejection while the co-shear flow layer in 3f traps the blob. The dynamics can be explained in terms of attraction (repulsion) of the blob and shear-layer charges. The sense of the flow shear in 3f is like the mean flow observed in NSTX (see Fig. 5); this sheared flow acts to enhance edge confinement.

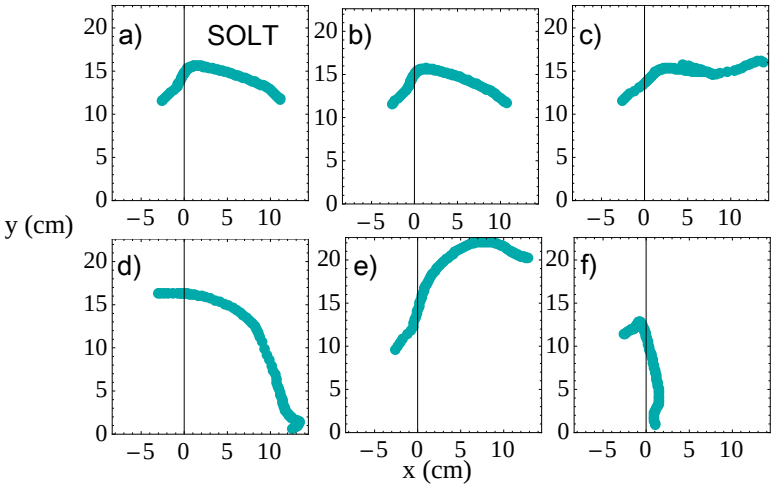

FIG. 3. SOLT seeded blob simulation tracks.

The acceleration a_y of the individual blob tracks is closely related to the fluid Reynolds stress.

$$\left\langle a_y \right\rangle = \left\langle \frac{dv_y}{dt} \right\rangle = \left\langle \mathbf{v}\cdot\nabla v_y \right\rangle = \frac{\partial}{\partial x}\left\langle v_x v_y \right\rangle \qquad (1)$$

where the quantities $\langle a_y \rangle$ and $\langle dv_y/dt \rangle$ are computed from averages of "single-particle" blob trajectories while $\left\langle \mathbf{v}\cdot\nabla v_y \right\rangle$ and $\partial_x \left\langle v_x v_y \right\rangle$ are regarded as statistically averaged fluid

quantities. The acceleration $\langle a_y \rangle$ was computed as a function of radial position by fitting smoothed curves to the trajectories x(t) and y(t) and then differentiating. This procedure was carried out on both experimental and simulation data and compared. Results are shown in Fig. 4.

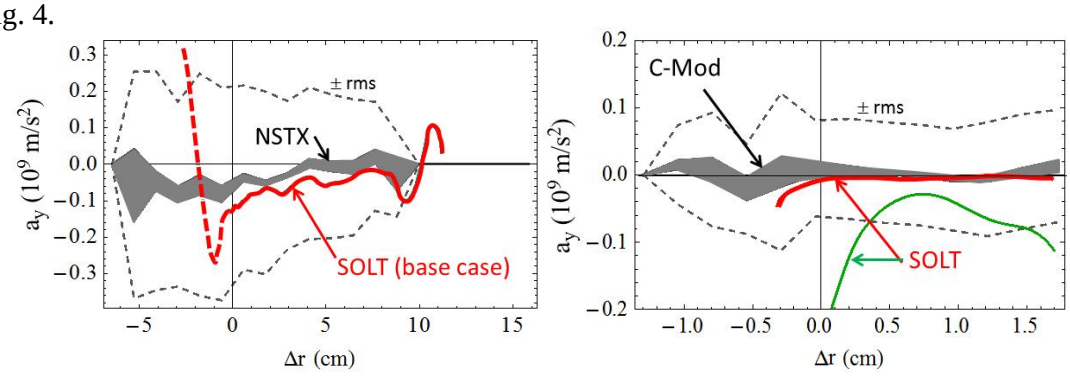

FIG. 4. Reynolds acceleration $\langle a_y \rangle$ for seeded blob simulations compared with experimental results for NSTX and Alcator C-Mod. The grey curves are experimental data. The central shaded region is the mean acceleration, with statistical uncertainty. The dashed grey lines show the mean ± rms deviations for the experimental data. Colored curves are from the SOLT seeded blob simulations. See text for explanation.

For the NSTX shot, the seeded blob simulation (red curve) does a remarkable job of modeling the experimentally observed mean acceleration, indicated by the thick grey region. (The red dashed portion of the NSTX simulation is the result of an unphysical initial transient as the seeded blob relaxes.) As for Fig. 3a, this blob was initialized with the mean blob parameters of Table I, and evolved using experimental outer midplane plasma profiles and parameters.

For the highly collisional Alcator C-Mod case, SOLT simulations are more challenging because collisionality is expected to allow the blob filaments to acquire structure (e.g. temperature gradients) along the magnetic field line. When seeded blob simulations were carried out for the C-Mod case using midplane values, and no flow damping, significant a_y resulted, as shown by the green curve in right panel of Fig. 4. The C-Mod experimental result of near-zero mean a_y could be modeled satisfactorily only by making several additional assumptions (red curve): complete parallel sheath disconnection in the SOL, partial collisional disconnection in the edge, and finite flow damping, $\nu/\Omega_i = 0.02$. Theoretically, in our model, flow damping is equivalent to friction and also to extra charge dissipation by cross-field currents. [4,5] The latter are expected when X-points (and their associated thin radial fans [19]) are present downstream along B. Friction could also be provided in this shot by neutral collisions [20]. With these simulation parameter choices, an acceleration is obtained that is close to the experimentally observed band.

Additional experimental confirmation of the Reynolds stress in these discharges can be ascertained by analyzing the elliptical deformations of the blob structure. We assume that the ellipticity and tilt angle of the blob electrostatic potential are similar to those of the density and temperature, and hence the GPI emission, notwithstanding the detailed differences in internal structure. (Recall that the blob density and temperature have a monopole structure, whereas the potential has a characteristic dipole structure [4,5]). Given this assumption, it can be shown that a normalized proxy for the RS, hereafter referred to as RSP is given by

$$\mathrm{RSP} = -\sin(2\theta)[1-(r_2/r_1)^2] \qquad (2)$$

where θ is the tilt angle (measured clockwise from the positive ΔR or x axis) and r_2 (r_1) is the major (minor) axis of the best-fit ellipse. In the absence of either ellipticity or tilt, there is no Reynolds stress.

Figure 5 (upper) shows the results of an RSP analysis for the NSTX and Alcator C-Mod shots. The spatial derivative $-\partial_x$ RSP is proportional to the Reynolds force. It follows that the mean Reynolds force for the NSTX shot is consistent with the observed direction of the mean blob flows in Fig. 5 (lower left). For the C-Mod shot, the mean Reynolds force is essentially zero, again consistent with the small flows observed in Fig. 5. A different analysis method of zonal flows for this (and other) Alcator C-Mod shots was described in Ref. [21] Small mean zonal flows were also reported for this C-Mod shot (1100824017), and the oscillating zonal flows were found to have a broadband frequency spectrum.

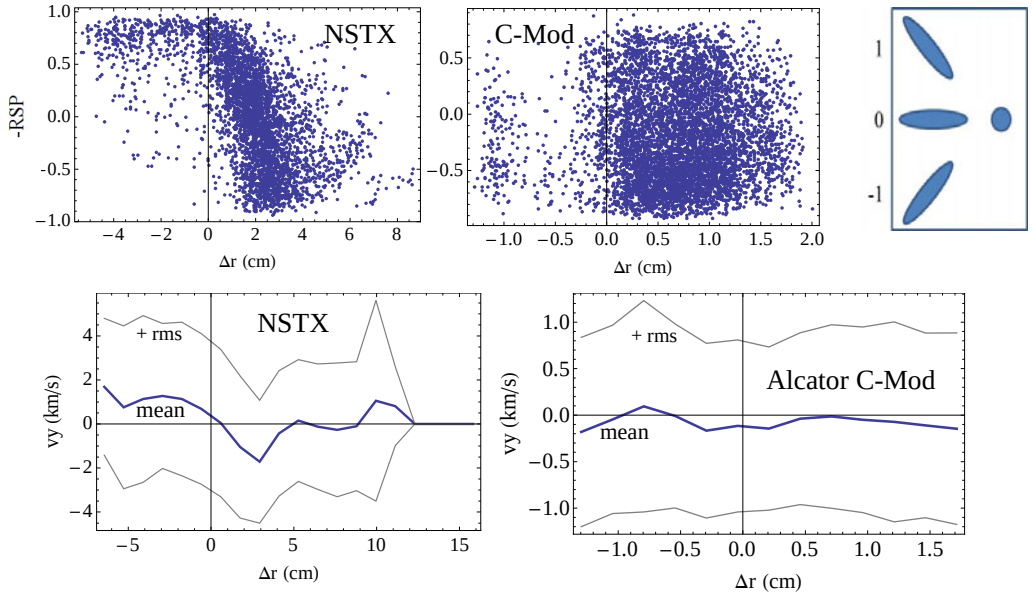

FIG. 5. Upper panels: proxy for the Reynolds stress for the NSTX and Alcator C-Mod shots obtained from experimental GPI data. Each dot is one blob shape. Far upper right: sketch of blob orientation for different values of the y-axis. Lower panels: thick blue line is the mean v_y of all blobs in the given radial bin. The thin gray lines above and below indicate the mean ± the rms deviation.

It is significant that for both the NSTX and C-Mod shots, an order unity variation of the RSP (essentially from -1 to 1, i.e. over the full possible range) is observed. This shows that significant instantaneous shearing stresses are acting on the blobs. In previous theoretical and simulation work [8] we have shown that order unity shearing deformations of the blob structure are consistent with the idea that shearing affects the blob dynamics, i.e. $\omega'_E \sim \gamma$ where γ is a characteristic linear growth rate or inverse auto-correlation time, and ω'_E is the shearing rate. When the shearing rate is of this magnitude or larger, it both creates isolated blob structures from radial streamers [8,22] and begins to suppress turbulent radial transport, e.g. consistent with the discussion of Fig. 3f. Qualitatively similar results to Fig. 5 were obtained from the SOLT turbulence simulations of these shots.

5. Conclusions

A combination of experimental data analysis, seeded blob simulations, and turbulence simulations (to be reported on elsewhere) have been used to study the interaction of blobs with sheared flows. Theoretical mechanisms related to radial inhomogeneity, and parallel

sheath currents from radial changes in magnetic topology cause the generation of Reynolds stress. An important conclusion is that these mechanisms are sufficient to explain the observed generation of blob poloidal flows (their size, radial scale, direction and reversal across the separatrix) in a low collisionality NSTX shot. A selected high collisionality Alcator C-Mod shot shows very small mean sheared flows. It was found that many characteristics of this shot could be simulated by additionally assuming (i) collisional disconnection of the midplane from the divertor sheaths, and (ii) flow damping or equivalently charge dissipation by radial currents, possibly due to X-point effects.

Acknowledgements

This work was supported by the US DOE under grants DE-FG02-97ER54392, DE-FG02-02ER54678, DE-AC02-09-CH11466, DE-FC02-99ER54512, DE-AC02-09CH11466, and PPPL Subcontract S009625-F.

References

[1] DIAMOND, P. H., et al., Plasma Phys. Control. Fusion 47 (2005) R35.

[2] DIAMOND, P. H. and KIM, Y.-B., Fluids B 3 (1991) 1626.

[3] TERRY, P. W. Rev. Mod. Phys. 72 (2000) 109.

[4] KRASHENINNIKOV, S. I., et al., J. Plasma Physics **74** (2008) 679.

[5] D'IPPOLITO, D. A., et al., Phys. Plasmas **18** (2011) 060501.

[6] ZWEBEN, S. J., et al., Nucl. Fus. **44** (2004) 134.

[7] LIPSCHULTZ, B., et al., Nucl. Fusion **47** (2007) 1189.

[8] RUSSELL, D. A., et al., Phys. Plasmas **16** (2009) 122304.

[9] RUSSELL, D. A., et al., Phys. Plasmas **14** (2007) 102307.

[10] SECHREST, Y., et al., Phys. Plasmas **18** (2011) 012502.

[11] ZWEBEN, S. J., et al., Phys. Plasmas **17** (2010) 102502.

[12] MYRA, J. R., et al., Phys. Plasmas **18** (2011) 012305.

[13] AGOSTINI, M., et al., Phys. Plasmas **14** (2007) 102305.

[14] SHESTERIKOV, I., et al., Nucl. Fusion **52** (2012) 042004.

[15] ALONSO, J.A., et al Plasma Phys. Control. Fusion **48** (2006) B465.

[16] DAVIS, W. M., et al., *54th Annual Meeting of the APS/DPP*, 2012, Providence, RI.

[17] FURNO, I., et al., Plasma Phys. Control. Fusion **53** (2011) 124016.

[18] MYRA, J. R., et al., Phys. Plasmas **11** (2004) 4267.

[19] FARINA, D., et al., Nucl. Fusion **33** (1993) 1315.

[20] KATZ, N., et al., Phys. Rev. Lett. **101** (2008) 015003.

[21] ZWEBEN, S. J., et al., Plasma Phys. Control. Fusion **54** (2012) 025008.

[22] BISAI, N., et al., Plasmas **12** (2005) 072520; and **12**, (2005) 102515.